

Locating acoustic emission with an amplitude-multiplexed acoustic sensor array based on a modified Mach–Zehnder interferometer

Jianmin Gong, J. M. K. MacAlpine, Wei Jin, and Yanbiao Liao

We report on an amplitude-division-multiplexed interferometric sensor array for locating acoustic emission. Preliminary experiments were carried out with a modified Mach–Zehnder interferometer consisting of two sensing arms and a reference arm and demonstrated a one-dimensional location accuracy of a few centimeters. The system can be extended for two- and three-dimensional location of acoustic emissions by the addition of one or two more sensing arms, respectively, in the interferometer. © 2001 Optical Society of America

OCIS codes: 060.2370, 060.4230.

1. Introduction

Locating acoustic emission is required for applications such as detecting cracks in structures, monitoring partial discharges in power transformers, and so on.¹ To locate the position of an acoustic source, several acoustic sensors placed in different locations are required. The time-delay differences between signals received by different sensors may be used to calculate the position of the acoustic source.²

Fiber-optic Mach–Zehnder interferometers have been applied to detect acoustic signals.^{1,3} The fiber-optic sensors have the advantages of immunity to electromagnetic interference and are particularly suited for measurement in environments with high-electromagnetic fields such as oil-filled power transformers.¹ A conventional Mach–Zehnder-type interferometer consists of a sensing arm containing a coiled acoustic sensor and a reference arm³ and allows only one acoustic sensor to be included within an individual interferometer.

One light source and one photodetector are required for operating each interferometer. The system cost is thus a multiple of that of a single Mach–Zehnder interferometer if a number of acoustic sensors are required.

Here we report on an amplitude-division-multiplexing technique that accommodates several acoustic sensors within a single modified Mach–Zehnder interferometer. All the sensors share the same reference arm, the same light source, and the same photodetector and thus allow a low-cost system for locating acoustic emission to be realized.

2. Principle

Figure 1 shows the proposed acoustic sensor array. A modified Mach–Zehnder interferometer consisting of N ($N = 2$ in Fig. 1) sensing arms and a reference arm is discussed here. The same principle can, however, be applied to other types of interferometer configuration. One acoustic sensor is located in each of the sensing arms. The acoustic sensors are fabricated by means of winding single-mode optical fibers around cylindrical tubes.^{1,3}

When a sound wave impinges on the sensing coil, the optical path length and hence the corresponding phase of light propagating along the fiber will change. The electrical field at the photodetector may be written as

$$E_t \equiv E_r + \sum_{i=1}^N E_i, \quad (1)$$

J. Gong (eejmgong@polyu.edu.hk) and Y. Liao are with the Electronic Engineering Department, Tsinghua University, Beijing 100084, China. J. Gong, J. M. K. MacAlpine, and W. Jin are with the Electrical Engineering Department, Hong Kong Polytechnic University, Hong Kong.

Received 26 February 2001; revised manuscript received 2 July 2001.

0003-6935/01/346199-04\$15.00/0

© 2001 Optical Society of America

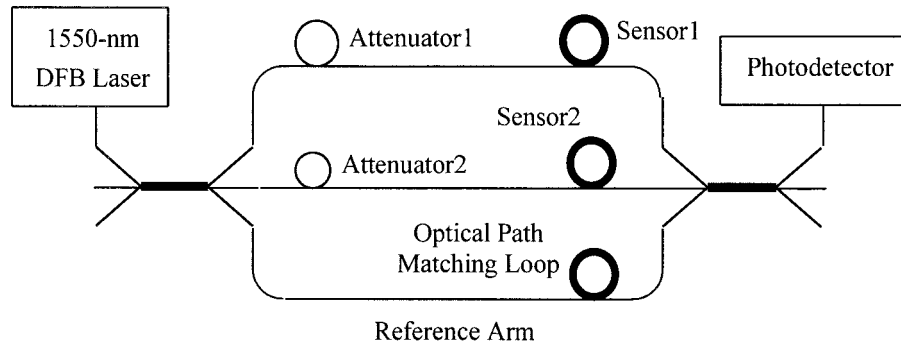


Fig. 1. Modified Mach-Zehnder interferometer. DFB, distributed feedback.

where E_r is the electrical field from the reference arm and E_i ($i = 1, 2, \dots, N$) is the field from the i th sensing arm. They can be expressed as follows,

$$E_i = E_{0_i} \exp(-j\phi_i), \quad (2)$$

$$E_r = E_{0_r} \exp(-j\phi_r), \quad (3)$$

where E_{0_i} , E_{0_r} and ϕ_i , ϕ_r are the amplitudes and phases of the respective electric fields. E_{0_i} and E_{0_r} depend on the coupling ratios of the input and the output couplers and the attenuation factors of individual sensing arms, and ϕ_i contains the phase variation induced by the acoustic wave impinging on sensor i .

The light intensity at the photodetector $I = E_t(E_t)^*$ may be divided into three categories:

1. Intensities of light signals from different arms (N sensing arms and one reference arm). These terms are not varying with acoustic disturbances and will not be discussed here.

2. Interferometric terms resulting from the coherent mixing between the signals from individual sensing arms and the reference arm. These terms may be written as

$$I_{ir} = 2 \sum_{i=1}^N E_i E_r \cos \theta_i \cos(\phi_i - \phi_r), \quad (4)$$

where a term $\cos \theta_i$ is included to account for the effect of polarization states within the i th sensing arm and the reference arm. The value of $\cos \theta_i$ will be zero if the polarization states from the two arms are orthogonal and will be maximized and equal to 1 if they are parallel.

3. The mixing terms between the signals from different sensing arms. These terms may be expressed as

$$I_{ij} = 2 \sum_{i=1, j>i}^N E_i E_j \cos \theta_{ij} \cos(\phi_i - \phi_j). \quad (5)$$

Again $\cos \theta_{ij}$ is included to represent the effect of polarization states.

As the polarization states in the fiber arms may vary with environmental disturbance, the value of $\cos \theta_i$, $\cos \theta_{ij}$ would vary with environment and could

cause the so-called signal fading in the interferometer output. This problem can be overcome by use of polarization-maintaining fiber or by insertion of depolarizers into the interferometer arms.⁴ The value of $\cos \theta_i$ (or $\cos \theta_{ij}$) will then become constant and equal to 1 and 0.707, respectively.

If the interferometer is designed such that $E_r \gg \max(E_i, E_j)$, I_{ij} will be significantly smaller than I_{ir} and can then be neglected. The remaining time-varying terms in the system output will then be given by Eq. (4). There are N terms in Eq. (4) corresponding to N independent sensing channels. The phase difference $\phi_i - \phi_r$ may be written as $\Delta\phi_i + \delta_i$, where $\Delta\phi_i$ is the phase shift induced by the acoustic signal, and δ_i is a slow, random, time-varying phase factor that is due to environmental effects. In the simple case in which all fiber within the sensing length L_i receives the same sound pressure P , the phase shift $\Delta\phi_i$ may be written as^{5,6}

$$\Delta\phi_i = n\eta k L_i P, \quad (6)$$

with

$$\eta \equiv -\frac{1-2\nu}{E} + \frac{n^2(1-2\nu)}{2E} (2p_{12} + p_{11}), \quad (7)$$

where $k = 2\pi/\lambda$; λ is the wavelength of light in free space; n is the refractive index of the fiber; and ν , E , p_{12} and p_{11} are, respectively, Poisson's ratio, Young's modulus, and strain-optic tensor elements of the optical fiber. Take silica optical fiber as an example: $n = 1.456$, $\nu = 0.17$, $E = 7 \times 10^{10}$ N/m², $p_{12} = 0.27$ and $p_{11} = 0.121$,⁶ and η can be calculated as -2.82×10^{-12} Pa⁻¹. For a segment of fiber with the length of 1 m, a pressure of 3.75×10^5 Pa will introduce 2π phase shift at the wavelength of 1550 nm.

When there is a sound burst,

$$P_0(t) = S(t) \text{rect}(t, 0, T), \quad (8)$$

where $\text{rect}(t, x, y)$ is a rectangular function whose value is 1 when $x < t < y$, and zero otherwise. The sound pressure at sensor i ($i = 1, 2, \dots, N$) will be

$$P_i(t) = \xi_i S(t - \tau_i) \text{rect}(t, \tau_i, T + \tau_i), \quad (9)$$

where ξ_i is a transmission loss factor and τ_i is the time delay. The sound pressure $P_i(t)$ will cause variation

in $\Delta\phi_i$ according to Eq. (6). If the value of L_i is large enough, $\Delta\phi_i$ can be made to vary by several multiples of 2π even for a moderate or weak sound pressure. Because of the periodic nature of the cosine function [Eq. (4)], this will result in a relatively higher frequency (compared with the sound signal) variation in the interferometer output.

If only the i th sensor receives the sound signal, then only the i th term in Eq. (4) will have a high-frequency component. The peak-to-peak value of this component will be $4E_r E_i$. For simplicity we have taken the value of $\cos \theta_i$ as 1. When two sensors, say, the i th and the j th sensors, receive the acoustic signal simultaneously, both the i th and the j th terms in Eq. (4) will contain high-frequency components. The peak-to-peak value of the composite signal will then be $4E_r(E_i + E_j)$. Similar results can be obtained for a number of sensors receiving the acoustic signals at the same time. However, different types of sound signals, e.g., different frequency, different source location, and different loss factor ξ_i , would affect only the phase and frequency contents of the interferometer output and have no effect on the amplitudes of the output signal. If the amplitudes of the different composite signals can be distinguished clearly, the change in the peak-to-peak value of the interferometer output may be used as a direct indication of which sensor or sensors are receiving signals and the time at which they start receiving the signals. The time-delay differences between the transitions can then be used to calculate the position of the acoustic source.

To distinguish the peak-to-peak values of the composite signals, the coupling ratio and/or the transmission loss of the sensing arms need to be tailored to ensure that different combinations of signals have different peak-to-peak values. For example, to locate an acoustic source along a straight line, a two-sensor array is needed. The values of E_1 and E_2 may be taken as 1 and 2. This gives three distinct peak-to-peak values, i.e., $4E_r$, $2 \times 4E_r$, and $3 \times 4E_r$, for the three possible combinations of signals. To locate an acoustic source within a plane, a three-sensor array has to be used; the values of E_1 , E_2 , and E_3 may be taken as 1, 2, and 4, and the corresponding peak-to-peak values will be $i(4E_r)$ ($i = 1, 2, 3, \dots, 7$) for the seven possible composite signals. Locating an acoustic source in a three-dimensional space requires the use of four acoustic sensors. The values of E_1 , E_2 , E_3 , and E_4 may be taken as 1, 2, 4, and 8; the corresponding peak-to-peak values will be $i(4E_r)$, with $i = 1, 2, 3, \dots, 15$ corresponding to the 15 possible combinations of the composite signals. E_i ($i = 1, 2$) may also be designed to take other values, as long as the peak-to-peak values of the composite signals do not repeat themselves.

3. Experiments and Discussion

Experiments were carried out with a modified, three-arm Mach-Zehnder interferometer. The interferometer was made from two 3×3 couplers. The optical path difference between any two of the arms

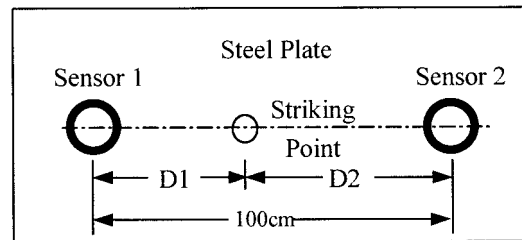


Fig. 2. Relative locations of acoustic sensor and acoustic source.

was controlled to be less than 10 cm. The light source used was a 1550-nm distributed-feedback laser diode with a coherence length of ~ 2 m. The two acoustic sensors (sensors 1 and 2) were made, respectively, by means of winding 7 and 5 m of single-mode optical fiber around cylindrical tubes with outer diameters of 1.5 cm. The power division ratios of both couplers were approximately 1/3. To distinguish signals from different acoustic sensors, a short segment of fiber in each of the sensing arms was bent to introduce additional loss. The bending radius in arm 2 was made smaller than that in arm 1 to ensure $E_1 > E_2$.

The sensor array was used to locate a sound disturbance along a straight line. The experimental arrangement is shown in Fig. 2. The two acoustic sensors were bound on a steel plate separated by a distance of 100 cm. A steel ball of 0.5 kg was dropped from a height of 50 cm to strike the plate to produce sound bursts. The striking position is in between and along the line that connects the two sensors. The distances from the striking point to sensors 1 and 2 are labeled D_1 and D_2 , respectively. Figure 3 shows a typical interferometer output, corresponding to the following setting: $D_1 = 81$ cm, $D_2 = 19$ cm.

As shown in Fig. 3, within a time period of 0–67.3 μ s, no acoustic signal was detected. The noise level was ~ 0.01 V peak to peak. This noise was due to the laser phase noise and can be reduced by means of carefully matching the optical path length between

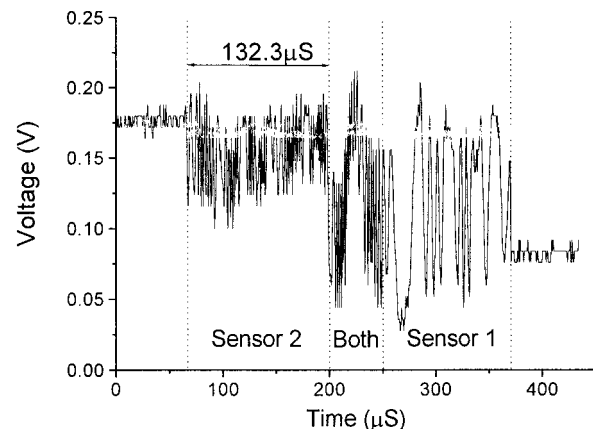


Fig. 3. Output signals for an acoustic source located at $D_1 = 0.81$ m and $D_2 = 0.19$ m.

the sensing and the reference arms. At the time of 67.3 μs the signal amplitude changes to ~ 0.06 V, indicating that sensor 2 was receiving the acoustic signal. The signal-to-noise ratio at that time is ~ 15.6 dB. After a time delay of ~ 132.3 μs , the amplitude changes to ~ 0.12 V, corresponding to the case in which sensor 1 and sensor 2 were receiving the acoustic signals at the same time. The signal-to-noise ratio at that time is ~ 21.6 dB. The ranges marked as sensor 2, both, and sensor 1 in Fig. 3 correspond to the cases in which just sensor 2, both sensor 1 and sensor 2, and just sensor 1 were receiving sound signals, respectively. Because the sound velocity in steel is ~ 5060 m/s,⁷ the time delay of 132.3 μs is equivalent to a distance difference of 66.9 cm. When we consider that the distance between the sensors is 1 m and that the sound source is located along a straight line between the two sensors, we can calculate that the distance from the striking point to sensor 2 was 16.55 cm. This result is close to the actual value of 19 cm.

The experiment was repeated for different striking positions along the line connecting the two sensors. The results are similar to that mentioned above with a maximum measurement error of less than 3 cm.

During the experiments no polarization-fading phenomena were observed. The interferometer was found to be stable with a peak-to-peak signal variation of less than 10% over a 2-h period.

It can be seen from Fig. 3 that the output signal has a different frequency when a different sensor is receives the acoustic signal. The signal frequency is higher when sensor 2, rather than sensor 1, receives the sound signal. This is because that sound source is closer to sensor 2, and the induced phase variation is larger by reason of larger acoustic pressure applied to sensor 2. When both sensors were receiving the sound signal at the same time, the output signal contained both frequency components. The exact frequency contents of the output signal would be affected by a number of factors such as the nature of the sound emission, the acoustic attenuation property of the materials, and the acoustic sensitivities of fiber sensing coils. This, however, should have no direct effect on the accuracy in locating the acoustic source.

The spatial resolution of the technique is decided by the accuracy in determining the difference in the start time of the sensor receiving the acoustic signal. Since the scheme is based on an amplitude-division-multiplexing technique, the time taken to reach a 2π phase shift (we call it start-up time here) or one cycle in output interferometric signal would be an important factor. Larger acoustic pressure and longer sensing fiber length reduce the start-up time and thus increase measurement resolution. Although our experiments demonstrated spatial resolution of ~ 3 cm, it is theoretically possible to achieve better resolution, even smaller than the diameter of the

sensing coil. If the acoustic pressure P_i is large enough, the induced phase shift could be larger than 2π even if only part of the sensing fiber interacts with the sound wave. This means that the start-up time could be less than the propagation time of the sound wave through the sensing coil, which would result in a spatial resolution that is smaller than that of the sensing coil.

As discussed in Section 2, we can extend the experiments to locate an acoustic source within a two- or a three-dimensional space by simply increasing the sensing arms to 3 and 4, respectively. If the pressure sensitivities of the different sensors are approximately the same, the best performance would be achieved by means of placing the sensors symmetrically around the possible acoustic emission. For the two-dimensional case the three sensors may be placed at the three vertices of the equilateral triangle that surrounds the sound source; and for the three-dimensional case the sensors may be located at the four vertices of the regular tetrahedron.

4. Conclusions

We have proposed what to our knowledge is a novel amplitude-division-multiplexed fiber-optic sensor array based on a modified Mach-Zehnder interferometer for locating acoustic emissions. The sensor array needs only one light source and one detector to address a multiarm interferometer and hence allow a simpler and more cost-effective measurement system to be realized. Experiments have been conducted with a two-sensor array for locating a sound source along a straight line and demonstrated a locating accuracy of better than 3 cm. The possibility of extending the present system to two- and three-dimensional measurements has also been discussed.

References

1. Z. Q. Zhao, J. M. K. MacAlpine, and M. S. Demokan, "Directionality of an optical fiber high-frequency acoustic sensor for partial discharge detection and location," *J. Lightwave Technol.* **18**, 795–806 (2000).
2. J. Tabrikian and H. Messer, "Three-dimensional source localization in a waveguide," *IEEE Trans. Signal Process.* **44**, 1–13 (1996).
3. J. A. Bucaro and H. D. Dardy, "Fiber-optic hydrophone," *J. Acoust. Soc. Am.* **62**, 1302–1304 (1977).
4. R. Ulrich, "Polarization and birefringence effects," in *Optical Fiber Rotation Sensing*, W. K. Burns, ed. (Academic, San Diego, Calif., 1994), pp. 31–80.
5. B. Budiansky, D. C. Drucker, G. S. Kino, and J. R. Rice, "Pressure sensitivity of a clad optical fiber," *Appl. Opt.* **18**, 4085–4088 (1979).
6. G. B. Hocker, "Fiber-optic sensing of pressure and temperature," in *Selected Papers on Single-Mode Optical Fibers*, A. Brozeit, K. D. Hinsch, and R. S. Sirohi, eds. (Society for Photo-Optical Instrumentation Engineers, Bellingham, Wash., 1994), pp. 440–443.
7. J. P. Cowan, *Handbook of Environmental Acoustics* (Van Nostrand, New York, 1994), p. 8.